HHS Public Access

Author manuscript

FASEB J. Author manuscript; available in PMC 2025 January 01.

Published in final edited form as:

FASEB J. 2024 January ; 38(1): e23358. doi:10.1096/fj.202301934R.

Hypoxia inducible microRNA-155 negatively regulates epithelial barrier in Eosinophilic Esophagitis by suppressing Tight Junction Claudin-7

Gary E Markey[1], **Sinéad Ryan**[1], **Glenn T Furuta**[2], **Calies Menard-Katcher**[2], **Eoin N McNamee**[3], **Joanne C Masterson**[1,2,*]

[1]Allergy, Inflammation & Remodelling Research Laboratory, Kathleen Lonsdale Institute for Human Health Research, Department of Biology, National University of Ireland Maynooth, Co. Kildare, Ireland.

[2]Gastrointestinal Eosinophilic Diseases Program, Digestive Health Institute, Children's Hospital Colorado, Department of Pediatrics, University of Colorado School of Medicine, CO, USA.

[3]Mucosal Immunology Research Laboratory, Kathleen Lonsdale Institute for Human Health Research, Department of Biology, National University of Ireland Maynooth, Co. Kildare, Ireland.

Abstract

MicroRNA (miRNA)-mediated mRNA regulation directs many homeostatic and pathological processes, but how miRNAs coordinate aberrant esophageal inflammation during eosinophilic esophagitis (EoE) is poorly understood. Here, we report a deregulatory axis where microRNA-155 (miR-155) regulates epithelial barrier dysfunction by selectively constraining tight junction CLDN7 (claudin-7). MiR-155 is elevated in the esophageal epithelium of biopsies from patients with active EoE and in cell culture models. MiR-155 localisation using *in situ* hybridisation (ISH) in patient biopsies, and intra-epithelial compartmentalisation of miR-155 shows expression predominantly within the basal epithelia. Epithelial miR-155 activity was evident through diminished target gene expression in 3D organotypic cultures, particularly in relatively undifferentiated basal cell states. Mechanistically, generation of a novel cell line with enhanced epithelial miR-155 stable overexpression induced a functionally deficient epithelial barrier in 3D air-liquid interface epithelial cultures measured by transepithelial electrical resistance (TEER). Histological assessment of 3D esophageal organoid cultures overexpressing miR-155 showed notable dilated intra-epithelial spaces. Unbiased RNA-sequencing analysis and immunofluorescence determined a defect in epithelial barrier tight junctions and revealed a selective reduction in the expression of critical esophageal tight junction molecule, claudin-7.

[*]**Correspondence should be addressed to:** Joanne C. Masterson, Allergy, Inflammation and Remodeling Research Laboratory, Kathleen Lonsdale Institute for Human Health Research, Department of Biology, Maynooth University, Maynooth, County Kildare, Ireland. Phone: 353.1.708.6369; Joanne.Masterson@mu.ie.

Author contributions

Study concept and design (JCM); acquisition of data or critical resources (GEM, SR, GTF, CMK); analysis and interpretation of data (GEM, ENM, JCM); drafting of the manuscript (GEM); critical revision of the manuscript for important intellectual content (GEM, SR, GTF, CMK, ENM, JCM); obtained funding (JCM).

Conflict of Interest Statement

Authors have declared that no conflict of interest exists.

Together, our data reveal a previously unappreciated role for miR-155 in mediating epithelial barrier dysfunction in esophageal inflammation.

Graphical Abstract

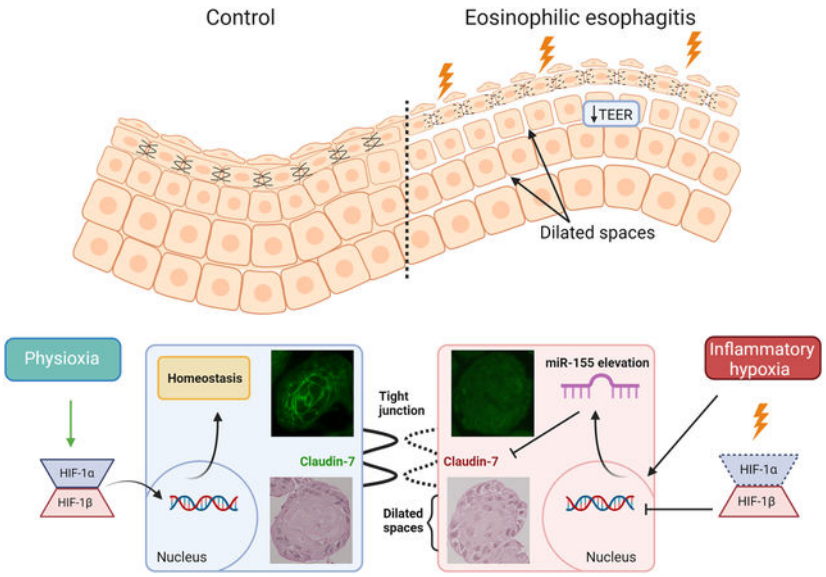

MicroRNA (miRNA)-155 is elevated in EoE patient esophagi. MiR-155 localisation using *in situ* hybridisation shows predominantly basal epithelial expression. Epithelial miR-155 activity was evident through diminished target gene expression, particularly in relatively undifferentiated basal cell states. MiR-155 stable overexpression induced a functionally deficient epithelial barrier in 3D air-liquid interface and organoid cultures, involving decreased tight junction Claudin-7 and elevated dilated intracellular spaces. Together, our data reveal a previously unappreciated role for miR-155 in mediating epithelial barrier dysfunction in esophageal inflammation.

Keywords

Barrier; Claudin 7; Eosinophilic esophagitis; Epithelium; Hypoxia; MicroRNA 155; miR-155; Tight junction

Introduction

Eosinophilic Esophagitis (EoE) is a chronic allergen-mediated disease of the esophagus characterised by extensive esophageal eosinophilia[1] and epithelial reactive changes, such as basal zone hyperplasia, dilated intracellular spaces, and epithelial barrier dysfunction[2,3]. The importance of the epithelium to pathophysiology has become central owing to a large body of research that has demonstrated the impact of the dysfunctional barrier in contributing to EoE pathophysiology[4–7]. This makes targeting epithelial healing as an attractive target for future therapeutic studies. Ultrastructural examinations in EoE has elucidated diminished intracellular junctions[8], and molecular studies identified important roles for IL-13 in contributing to the loss in epithelial integrity in EoE[4,7]. Our previous work has demonstrated the action of elevated TGF-β1, a pleiotropic growth factor, in contributing

to epithelial barrier dysfunction by attenuating the key tight junction molecule claudin-7 in EoE[9]. Thus, a better understand of the key potentiators of the heterogenous pathological epithelial microenvironment is critical in the context of EoE.

MicroRNAs (miRNAs) are a class of small endogenous RNA molecules between 18 and 25 nucleotides long, which function primarily in the posttranscriptional regulation of mRNA targets[10]. Previous research has defined a distinct global miRNA profile in active EoE, and subsequent molecular studies have particularly focused on their roles in immune regulation and responses to therapeutic intervention[11–15]. Elevated expression of pro-inflammatory miRNAs miR-223, miR-21, and miR-146a/b correlated with esophageal eosinophilia and invading leukocytes[11–14]. Several studies have shown the overlap in miRNA expression patterns in EoE patients[11–13], however the exact function miRNAs exert on the esophageal epithelium in EoE pathophysiology has yet to be fully elucidated.

One such underexplored miRNA in the context of EoE is miR-155[16]. MiR-155 exists with two arms originating from the precursor miRNA(pre-miRNA), miR-155–3p and miR-155–5p with only one of these arms possessing functional dominance and the remaining strand is degraded[17]. Mature miR-155–5p (called miR-155 here after) is considered the dominant arm that is retained and primarily understood for its pro-inflammatory role in chronic immune-mediated pathologies, such as inflammatory bowel disease (IBD)[18], allergic asthma[19,20], allergic rhinitis[21], and psoriasis[22,23]. Further studies in a mouse model of atopic dermatitis showed that allergen-induced miR-155 elevation negatively regulated tight junction expression through the attenuation of protein kinase inhibitor α (PKIα) in skin epithelia[24]. MiR-155 was previously listed as a significantly increased miRNA in whole biopsies of EoE patients[13], however its source and function has not been explored. MiR-155 has been shown as a potent hypoxia responsive miRNA capable of destabilization of *HIF1A* mRNA[18,25,26], as well as contributing to barrier dysfunction in a range of cell types[18,24,27]. MiR-155 has been previously researched as a pro-inflammatory miRNA and key in promoting the type-2 immune response in atopy[19,20,28].

The intercellular tight junctions have emerged as key regulators of epithelial barrier in the esophagus. Our previous research has demonstrated the key role of claudin-7 in barrier defects in EoE, which is dysregulated by TGF-β1 expression[9]. In addition we showed attenuated tight junction expression of claudin-1 mediated by dysregulation of the hypoxia responsive transcription factor HIF1-α in EoE[29]. Others have shown that tight junctions are dysregulated in EoE patients[30], while mechanistic studies indicate this may occur in response to inflammatory mediators such as TLR2-signlaing, IL-9 and IL-13[31–33]. Although miR-155 expression has been detected in EoE in a microarray screen study[13], the full impact of altered miR-155 expression on the allergic esophageal epithelium as it relates to esophageal barrier function has yet to be fully understood. Here we elucidated the cellular source of miR-155 is within the esophageal epithelium and is most expressed in basal epithelia. We determined a number of target genes that are altered in esophageal epithelial cells, including *HIF1A* in the hypoxic EoE microenvironment. We defined the role of miR-155 in contributing to esophageal barrier dysfunction. Thus, we propose that miR-155 is elevated in the esophageal epithelium of patients with EoE and contributes to epithelial barrier dysfunction through regulation of tight junction *CLDN7* expression.

Materials and Methods

Human Subjects

Research participants between 4–17 year of age underwent clinically indicated upper endoscopy and mucosal biopsy at Children's Hospital Colorado were included in this study as part of an IRB ethically approved study. Informed consent and assent when applicable was received in writing prior to research participation. Inclusion criteria based on clinical review of patient records, participants were categorised into uninflamed controls, active EoE, and inactive EoE. Uninflamed control individuals underwent upper endoscopy for symptoms of abdominal pain, feeding difficulty, and diarrhoea and had normal esophageal histology with 0 eosinophils per high power field (eos/HPF). Active EoE individuals had ≥15 eos/HPF and displayed symptoms of esophageal dysfunction, as well as abdominal pain, dysphagia, poor weight gain, and vomiting. Inactive EoE individuals had a previous diagnosis of EoE and underwent treatment with topical corticosteroids or elimination diet with resolution of symptoms and displayed <15 eos/HPF. Clinical features including diagnosis, age, sex, and peak eosinophils per HPF (Table 1). Esophageal biopsies were placed in 10% neutral buffered formalin for paraffin embedding, sectioning, and staining.

Cell culture and 3D-Air-Liquid Interface

Human EPC2-hTERT, miR-155OE (EPC2-hTERTs stably overexpressing miR-155–5p), control cells (EPC2-hTERT negative controls), Claudin-7 knockdown (Claudin-7KD) and shRNA control cells[9] were cultured in keratinocyte serum-free media (KSFM) (Thermo Scientific) supplemented with Bovine Pituitary Extract (BPE), human Epidermal Growth Factor (Thermo Scientific) as demonstrated previously[9,29].

The response of cells to extended experimental hypoxia were cultured for mRNA (12-well plate), whole cell protein (6-well plate in duplicate), and nuclear protein (T75). Twenty-four hours post-seeding, KSFM was replaced with preconditioned KSFM which was either normoxic (21% O_2) or hypoxic (1% O_2). Cells were cultured in either normoxia (21% O_2) or hypoxia (1% O_2) for 0, 4, 24, 48, and 72-hours for analysis.

The 3-dimensioanal air-liquid interface (3D-ALI) model was used, as previously reported[9,29,34]. In brief, cells were cultured and submerged in KSFM (Thermo Scientific) without antibiotics and grown to confluence on 0.4μm semi-permeable 6-well transwell inserts (Corning) for 2 days. When cells reached confluence, on day 2, KSFM was replaced with high calcium KSFM (Ca^{2+}=1.8mM) for 5 days to terminally differentiate the cells. After 5 days in high calcium KSFM, media was then removed from the upper chamber which exposed the cells to the air liquid interface for a further 4 days which allowed the stratification process to begin.

Epithelial barrier was assessed using transepithelial electrical resistance (TEER) with an Ohmmeter (World Precision Instruments). *In vitro* measurements of barrier by TEER were carried out at day 7, 9, and 11 on EPC2-hTERT, miR-155OE, and control cells. At the end of the 3D-ALI culture, cells were harvested for miRNA, mRNA, and protein expression analysis.

Generating a lentivirus-mediated stable miR-155–5p overexpressing cell line

For the generation of a stable overexpressing miR-155–5p cell line, EPC2-hTERT cells were transduced with MISSION Lenti microRNA hsa-miR-155–5p TRC2-pLKO-puro construct (HLMIR0254; Merck), and MISSION Lenti microRNA TRC2-pLKO-puro negative control construct (NCLMIR001; Merck). In brief, EPC2-hTERT cells were cultured to appropriate confluence in a 6-well plate. Once cells reached confluence, 1mL of pre-warmed KSFM containing 16μg of polybrene (Merck) was added followed by the appropriate TRC2-pLKO-puro construct for 24 hours at 37°C. The transduction solution was then removed and fresh KSFM was added to allow the cells to recover. When cells reached 70% confluence, the selection of stable integration was started by introducing 0.3μg/mL of puromycin (Merck) into the KSFM. After the selection process, the cell lines were cultured and expanded as normal for later analysis.

Esophageal epithelial organoid cultures

Esophageal epithelial organoid cultures were generated from miR-155OE, control cells, Claudin-7KD, and shRNA control cells. Briefly, cells were counted and placed into a 1:1 ratio of cold Matrigel (Corning) and 0.6mM Ca^{2+} KSFM. Organoids were seeded onto a pre-warmed Nunclon surface 48well plate (Thermo Scientific) in 25μL domes with one dome per well each containing 1,000 organoids. The plate was then inverted to allow proper Matrigel dome formation and incubated at 37°C for 20 minutes before the addition of 300μL of KSFM-containing 0.6mM Ca^{2+}. Organoid media was changed every second day with KSFM containing 0.6mM Ca^{2+} for 11 days in total as per the literature[35]. Six wells of organoids were seeded each for mRNA/miRNA, protein, and histology which were pooled on day 11 for isolation. Isolation of organoid cultures began with the dissociation of Matrigel domes using dispase (Corning), as well as a series of PBS wash steps and centrifugation to purify the harvested organoids.

Following these wash steps miRNA/mRNA and protein isolation was carried out as described in this manuscript. Organoids isolated for histology were first fixed in 4% paraformaldehyde (PFA) (Fisher Scientific) overnight at 4°C before encapsulation in a 2% bacto agar (#214010, Fisher Scientific), 2.5% Gelatin Type-B (#G7–500, Fisher Scientific) dome. Organoids were then placed in 70% ethanol overnight followed by normal tissue processing into FFPE blocks.

mRNA/miRNA isolation and quantitative RT-PCR

Total RNA or separated fractions of miRNA and mRNA were isolated from esophageal epithelial cells using TRIzol Reagent and the RNeasy kit according to the manufacturer's instructions (Qiagen). Nucleic acid concentration was measured using a NanoPhotometer N60 spectrophotometer (Implen). cDNA synthesis and RT-PCR was performed using the miRCURY LNA RT Kit (miRNA) (Qiagen) and miRCURY LNA miRNA PCR assay (Qiagen) or the high-capacity cDNA archive kit (mRNA) (Applied Biosystems) with PrimeTime predesigned qPCR primers (IDT) as per manufacturer's instructions. Real-time qRT-PCR was performed using an Applied Biosystems Step One Plus real time PCR machine, and data were normalised to SNORD48 (miRNA) or 18S (mRNA) and were calculated as relative quantity using the $2^{-\Delta\Delta Ct}$ method, where Ct is the cycle threshold.

RNA extraction, library preparation and sequencing

RNA sequencing and differential gene expression analysis was performed by Novogene Europe ltd. In brief, total RNA was isolated from control and miR-155OE 3D-ALIs using the RNeasy kit (Qiagen) as per the manufacturer's instructions. Directional paired-end mRNA sequencing was carried out using the NEB Next® Ultra RNA Library Prep Kit for Illumina® (Cat No. 7530), with PE150 sequencing on a NovaSeq 6000 using an S4 flow cell prepared with the Illumina 300 cycle Reagent Kit (v1.5) by Novogene Europe ltd. Prior to sequencing all RNA samples passed quality control for quantitation, integrity, and purity prior to and during library preparation. Differentially expressed data was assessed for statistical significance using Benjamini-Hochberg false discovery rate to determine differential gene expression in which an FDR ≤0.1 was considered significant. RNA sequencing data was uploaded to the GEO repository under accession GSE244629.

Western blotting and densitometry

Nuclear protein isolates were isolated using NE-PER Nuclear Extraction Reagents per manufacturer's instructions (Thermo Scientific). Whole-cell protein was harvested in RIPA buffer containing Roche cOmplete Mini Protease Inhibitor Cocktail (Sigma-Aldrich).

Electrophoresis was carried out on polyacrylamide gels. Membranes were blocked and probed with primary antibody overnight and incubated with appropriate HRP-conjugated secondary antibodies for 1 hour at room temperature. Visualisation of western blots was carried out using chemiluminescent detection (WesternBright ECL- HRP Substrate, MyBio Ltd, SuperSignal West Pico PLUS, Thermo Scientific, SuperSignal West Femto, Thermo Scientific), and visualised using the ChemiDoc MP Imaging System (Bio-Rad), with densitometry conducted on the Bio-Rad Image Lab software normalised to the appropriate housekeeper.

Primary antibodies used included HIF-1α monoclonal mouse antibody (#610959, clone 54, BD Biosciences), claudin-1 polyclonal rabbit antibody (#51–9000, Invitrogen), claudin-4 monoclonal mouse antibody (#sc-376643, clone A-12, Santa Cruz Biotechnology), claudin-7 polyclonal rabbit antibody (#34–9100, Invitrogen), TATA-binding protein mouse monoclonal (#MA1–21516, clone 1TBP18, Invitrogen), β-Actin polyclonal rabbit antibody (#A5060, Merck), and GAPDH monoclonal mouse antibody (#SC-32233, clone 6C5, Santa Cruz Biotechnology).

In situ hybridization of miR-155 on patient biopsies

In situ hybridization was performed on FFPE sections obtained from controls, patients with active EoE, and patients with inactive EoE using the RNAscope 2.5 HD assay (#322300, ACD Bio) and the hsa-miR-155 host gene probe (miR-155HG) (#450341, ACD Bio). ISH was performed as per manufacturer's instructions. ImageJ was used to quantify the number of cells present in the tissue, and to quantify the abundance of miR-155HG punctates. Specific compartmental analysis of miR-155 abundance within each of the basal, suprabasal, and superficial layers of the epithelium was quantified per cell using ImageJ trainable weka segmentation in a manner blinded to specimen information. Compartmental epithelial miR-155 punctates were pooled to obtain total epithelial miR-155 counts.

Immunofluorescent Staining

FFPE esophgeal organoids were cut into 3 μM sections and stained with hematoxylin and eosin (H&E). Immunofluorescent staining was performed on 2 μM FFPE organoid sections. Samples were deparaffinized via sequential immersion with xylene followed by graded ethanol immersion and rehydration. Heat induced antigen retrieval in sodium citrate buffer (Vector Laboratorie) was used. Sections were blocked in 5% bovine serum albumin in tris-buffered saline for 30 minutes. Primary antibodies claudin-7 (1:100, polyclonal rabbit antibody (#34–9100, Invitrogen)), keratin-14 (1.1500, polyclonal chicken antibody (#906004, Biolegend)), keratin-4 (1:100, monoclonal rabbit antibody (clone EP1599Y, #ab51599, abcam). Slides were incubated at 4°C overnight. Slides were washed and incubated for 1 hour at room temperature in secondary antibody of Alex Fluor 488 Goat anti-rabbit IgG, Alexa Fluor 568 Goat anti-rabbit IgG or Alexa Fluor 568 Goat anti-chicken IgG (Invitrogen). Slides were washed, counterstained with DAPI and mounted for visualization.

Statistical analysis

Statistical analysis of data was performed using a students' t-test, ordinary one-way ANOVA, or Kruskal-Wallis tests with Dunn's correction for multiple comparisons. A minimum of 3 independent repeats (n=3) were conducted for each experiment. Data are presented as means ± SEM. A P-value less than or equal to 0.05 was considered statistically significant within this study. Higher levels of significance are noted in some cases; $*P \leq 0.05$, $**P \leq 0.01$, $**P \leq 0.001$.

Results

MiR-155 is elevated in active EoE patient biopsies and most active in immature epithelia during stratification at 3D-ALI.

To understand the cellular source and expression levels of miR-155 in esophageal health and following allergic inflammation, its expression and localisation was investigated via *in situ* hybridisation (ISH) in esophageal biopsies from a cohort of uninflamed controls and compared to patients with active EoE, and inactive EoE. Examination showed punctate localisation of miR-155 within epithelial cells, with increased overall expression in patients with active EoE. This was particularly evident within the basal and suprabasal epithelium of active EoE (Figure 1A inset). Histomorphometric compartment specific quantification of epithelial miR-155 found that active EoE had significantly higher expression within the basal layers of the epithelium when compared to uninflamed controls (10.45 ± 0.95 vs 4.10 ± 0.92, active EoE vs uninflamed control, p≤0.05). MiR-155 abundance was significantly lower in the basal esophageal epithelium of inactive EoE patients (2.26 ± 0.84 vs 10.45 ± 0.95, inactive EoE vs active EoE, p≤0.01) (Figure 1A and B). Elevated miR-155 was also observed in the suprabasal epithelium of active EoE versus uninflamed controls (5.03 ± 0.59 vs 1.71 ± 0.35, active EoE vs uninflamed control, p≤0.05) along with a significant decrease in miR-155 in inactive EoE versus active EoE (0.77 ± 0.34 vs 5.03 ± 0.59, inactive EoE vs active EoE, p≤0.01) (Figure 1A and B). A modest yet non-significant elevation of miR-155 in the superficial epithelium of active EoE versus uninflamed controls was detected, however the superficial compartment between active EoE and inactive EoE showed a loss of miR-155

in the superficial epithelium in patients with inactive disease (5.01 ± 0.41 vs 0.97 ± 0.4, active EoE vs inactive EoE, p≤0.001) (Figure 1B). Total epithelial miR-155 was elevated in active EoE patients versus uninflamed controls (20.49 ± 1.33 vs 7.68 ± 1.37, active EoE vs uninflamed control, p≤0.05), as well as a significant decrease in inactive EoE versus active EoE (3.85 ± 1.54 vs 20.49 ± 1.33, inactive EoE vs active EoE, p≤0.01) (Figure 1C)

In light of the accumulation of miR-155 in the basal and suprabasal epithelial layers in patients with active EoE, we endeavoured to recapitulate these findings *in vitro*. MiR-155 transcript product and a number of its target genes were examined throughout a time course culture in organotypic 3-dimensional air liquid interface (3D-ALI). We hypothesised that miR-155 expression would gradually decrease during *in vitro* stratified squamous epithelial maturation from an initial submerged immature basal-like population harvested on day 2 (D2), on towards the continuum of differentiation to a suprabasal-like population harvested on day 7 (D7), and finally a terminally differentiated stratified epithelium harvested on day 11 (D11) (Figure 1D). MiR-155 expression was highest in immature epithelia on D2 (0.91 ± 0.04, p≤0.05) and D7 (0.8 ± 0.2, p≤0.05) with abrogation of expression in more mature epithelial cells on D11 (0.2 ± 0.05, p≤0.05) in accordance with terminal differentiation observed in the 3D-ALI model system. To confirm functionality of miR-155 on mRNA regulation, qRT-PCR was performed on a selection of miR-155 targets which were defined using both *in silico* predicted (TargetScan[36]) and functionally validated (miRTarBase[37]) databases with some chosen targets having notable functions within the esophageal epithelium (Figure 1E). MiR-155 targets displayed inverse relationships at 3D-ALI, whereupon in the reduction of miR-155 on D11 an elevation of target genes was observed including *PTEN* (2.65 ± 0.18, p≤0.0001), and tight junction molecules *TJP1* (1.53 ± 0.15, p≤0.01), and *OCLN* (34.3 ± 4.2, p≤0.001). There was a selectivity to this functionality where not all selected target genes assessed followed this inverse relationship, for example *WEE1*. However, a commonly researched miR-155 target *CLDN1* was significantly elevated in the absence of miR-155 (119.2 ± 22.8 p≤0.05) in this 3D-ALI model at D11 (Figure 1E). Together these data have showed that miR-155 is present and elevated in the esophagus of patients with EoE (Figure 1A, B, C) and is capable of being produced both *in vivo* and may be most functional *in vitro* in immature epithelial cells in stratified squamous inducing 3D-ALI culture.

MiR-155 is a hypoxia responsive miRNA that displays an inverse relationship with its target HIF-1α when cultured in extended experimental hypoxia.

Our previous research in EoE showed that there was an increase in the hypoxic constraints within the esophagus during EoE, contributed in part due to elevated oxygen consumption and thus competition from invading activated eosinophils[29]. This sustained and elevated esophageal hypoxia led to the paradoxical loss of HIF-1α signaling in EoE and resulted in the dysregulation of epithelial barrier dysfunction via the selective decrease in CLDN1. *In silico* database search and literature search highlighted miR-155 as a suppressor of *HIF1A* mRNA (Figure 2A). Thus we sought to investigate the relationship between hypoxic stress and miR-155 *in vitro* using a humidified hypoxia chamber. We hypothesised that prolonged experimental hypoxia would increase the expression of miR-155–5p arm specifically (hereafter miR-155). Esophageal epithelial cells were cultured in experimental hypoxia (1%

O_2) and compared to normoxic (21% O_2) controls over a prolonged time course up to 72-hours. qRT-PCR was performed from isolated miRNA to investigate whether miR-155 was responsive to extended experimental hypoxia in esophageal epithelial cells. MiR-155 underwent a significant increase over time commencing at 24-hours in hypoxia (1.98 ± 0.2, $p \leq 0.05$) and increased further at prolonged timepoints of 48-hours (2.54 ± 0.4, $p \leq 0.01$), and 72-hours (2.13 ± 0.2, $p \leq 0.01$) (Figure 2B). The expression of miR-155–3p was also investigated via RT-PCR in response to extended hypoxia but found that in accordance with the literature and our hypothesis that the 3p arm was not detectible in EPC2-hTERT cells. As our previous work has shown[29], *HIF1A* expression peaks at the acute 4-hour period in hypoxia (1.32 ± 0.1, $p \leq 0.05$) and steadily decreased throughout 24-hours (0.7 ± 0.04, $p \leq 0.01$), 48-hours (0.58 ± 0.1, $p \leq 0.05$), and 72-hours (0.36 ± 0.06 $p \leq 0.001$) at hypoxia (Figure 2B). This expression profile is inverse to that of miR-155.

To confirm the inverse relationship between miR-155 and *HIF1A* an inverse linear regression analysis was performed (Figure 2B). This showed that while miR-155 was elevated during timepoints of prolonged experimental hypoxia (48 and 72-hours), *HIF1A* was highest during more acute timepoints (4-hours). This inverse relationship between *HIF1A* and miR-155 was statistically significant ($p \leq 0.01$, $R^2 = 0.75$) (Figure 2B). Although *CLDN1* has previously been validated as a miR-155 target, linear regression did not show a statistically significant inverse relationship ($p=0.4$, $R^2 = 0.1$). Furthermore, extended experimental hypoxia diminished functional nuclear HIF-1α protein expression in esophageal epithelial cells (Figure 2C), and displayed no observable impact on *HIF2A* or *HIF1B* (Figure 2D). Extended experimental hypoxia was shown to have no inhibitory effect on the miRNA processing genes *DROSHA* and *DICER,* as well as having no negative impact on the key RNA induced silencing complex (RISC) gene *AGO2* (Figure 2E). These data confirmed the inverse relationship between esophageal epithelial *HIF1A* and miR-155, as well as the maintenance of functional miRNA machinery in the pathologically hypoxic EoE microenvironment.

Augmented overexpression of esophageal epithelial cell miR-155 leads to epithelial barrier dysfunction.

To further understand previously unexplored molecular and functional consequences of elevated miR-155 in the esophageal epithelium, independent of the complexities of experimental hypoxia, we generated a stable miR-155 overexpressing (miR-155OE) EPC2-hTERT cell line using lentiviral-mediated transduction and confirmed a significant overexpression of miR-155 at baseline (Figure 3A). qRT-PR analysis of *in silico* and functionally validated miR-155 targets was performed on miR-155OE cells in submerged culture. This confirmed attenuated *HIF1A* expression relative to control (0.87 ± 0.02 vs 0.62 ± 0.05, Control vs miR-155OE, $p \leq 0.05$), *CLDN1, PTEN, WEE1,* and *TJP1* showed no change in miR-155OE cells, however *OCLN* did display a significant reduction (0.95 ± 0.03 vs 0.58 ± 0.13, $p \leq 0.05$) in miR-155OE cells (Figure 3A). This suggests the importance of organotypic culture and microenvironmental cues to appropriate miR-155 function.

To better recapitulate the stratified squamous physiology of the esophageal epithelium *in vitro* and to discern what impact the overexpression of miR-155 has on esophageal

epithelial barrier, miR-155OE cells were cultured in 3D-ALI. Functional epithelial barrier assessment by way of transepithelial electrical resistance (TEER) was conducted to evaluate the differences in epithelial barrier between miR-155OE and control cells. A significant decrease in barrier as measured by TEER (549.4 ± 18.3 vs 441.6 ± 25.0 ohms.cm^2, Control vs miR155OE, p≤0.01) was found in miR-155OE cells when compared to control cells (Figure 3B). H&E staining of these cells at 3D-ALI showed a prominent perturbation of miR-155OE cell stratification when compared to controls, which displayed normal stratification (Figure 3C). From this data it was hypothesised that the overexpression of miR-155 induced a functionally deficient epithelial barrier via the negative regulation of barrier-associated genes. Next, qRT-PCR analysis of a selection of EoE-relevant transmembrane epithelial barrier molecules associated with tight junctions, adherens junctions and desmosomes was performed[9,14,29,32,38], some of which have been previously published as miR-155 targets in other epithelia (via miRTarBase[37]) (*CLDN1, DSG2, TJP1*). Interestingly, we found that among the barrier molecules we tested, tight junction *CLDN7* was the only molecule that was selectively and significantly downregulated in association with miR-155 overexpression in esophageal epithelial cells at 3D-ALI (0.95 ± 0.01 vs 0.65 ± 0.1, Control vs miR-155OE, p≤0.05) (Figure 3D). Western blotting of the primary claudins expressed within the esophageal epithelium correlates with qRT-PCR data where a significant decrease in claudin-7 was observed (0.75 ± 0.06 vs 0.58 ± 0.03, Control vs miR-155OE, p≤0.05) (Figure 3E). Interestingly, no difference in the expression of claudin-1 was seen, despite it being a validated target of miR-155 in other epithelia. These data confirm a functional consequence of elevated miR-155 in regulating barrier dysfunction via decreased *CLDN7*.

Overexpression of miR-155 regulates gene expression profiles associated with EoE-like epithelial dysfunction.

In order to explore other mediators and possible roles of miR-155 in esophageal epithelia, unbiased RNA sequencing was performed on miR-155OE cells and controls following culture at 3D-ALI. A significance cut-off of FDR ≤0.1 yielded 1,026 significantly upregulated genes, and 627 downregulated gene signatures (Figure 4A). Downregulated genes included *ACTN1,* involved in cytoskeleton organisation, as well as *CTNNAL1* and *SPINK7* which has previously been shown to regulate the loss of barrier integrity in EoE[39]. The suprabasal cytokeratin, *KRT4* was significantly reduced in miR-155OE cells, as well as the tight junction *CLDN23* (Figure 4A). Conversely, RNA sequencing showed a significant elevation in the diagnostically attractive collagen *COL8A2,* as well as increases in *CDH26, EPPK1, MYL4,* and *MMP9* which have been previously identified in EoE transcriptomics[40] (Figure 4A).

In order to further understand the impact of miR-155 overexpression on esophageal dysfunction, we performed gene ontology analysis (GO). Amongst the most highly upregulated GO pathways were UV response, and frizzled binding (GO: 0005109). The top ten downregulated pathways enriched by GO analysis were involved in cytoskeleton (GO:0005856), supramolecular fiber organization (GO: 0097435), focal adhesion (GO: 0005925), and cell-substrate junction (GO: 0030055) (Figure 4B). Importantly, these pathways share commonalities in overall epithelial cell organisation and are important

precursors in functional barrier formation, which has been shown to be dysfunctional in EoE pathogenesis[7]. In order to further investigate the action of miR-155OE as it relates to EoE pathology the miR-155OE interactome was compared with a publicly available RNA sequencing dataset of inflammatory EoE patients (GSE: 197702)[41]. An expanded volcano plot of the genes identified in GO:00005856, cytoskeleton was generated (Figure 4C). Downstream analysis of the differentially regulated genes shared between that of the miR-155OE and EoE transcriptome yielded on overlap of 167 genes (Figure 4D). Of these 167 genes, there included an assortment which have previously been investigated in the pathogenesis of EoE and which were differentially regulated in our RNA sequencing (Figure 4D (left)). Comparative disease analysis of these overlapping genes showed enrichment for Clouston syndrome, Netherton syndrome, Palmoplantar keratosis, and EoE highlighting the perturbed epithelial function common between these diseases (Figure 4D (centre)). GO cellular component analysis of these 167 differentially regulated genes were enriched for Intermediate Filament/Cytoskeleton (GO:0005882)/(GO:0045111), and Keratin Filament (GO:0045095) (Figure 4D (right)), from which five differentially regulated genes, *KRT4, PKP2, EPPK1, PHLDB2,* and *KRT78* were primarily enriched and have been shown to be involved in EoE pathogenesis (Figure 4E).

Further validation of dysregulated KRT 4 mRNA in miR-155OE organoids was confirmed by qRT-PCR, confirming a decrease in *KRT4* (0.96 ± 0.003 vs 0.20 ± 0.01, Control vs miR-155OE, p≤0.001). In addition, an increase in the expression of inflammation associated keratin-16 (*KRT16*) (0.98 ± 0.006 vs 2.63 ± 0.23, Control vs miR-155OE, p≤0.01) (Figure 4F). Finally, immunofluorescent staining of basal marker keratin-14 (KRT14) showed no change, but analysis of suprabasal keratin-4 (KRT4) showed decreased and more diffuse intensity of the suprabasal Keratin 4 (Figure 4G). Together these data support our RNA sequencing, RT-PCR and *in silico* analysis in showing a difference in cytoskeletal arrangement, and in particular KRT4, between control and miR-155OE cells in organoid cultures.

MiR-155 overexpression in esophageal organoid cultures confirm CLDN7 tight junction attenuation and phenocopies dilated intracellular spaces in EoE.

Next to investigate the impact of miR-155 overexpression, miR-155OE cells were subjected to differentiating 3D organoid cultures for 11 days. Based on functional TEER data showing decreased barrier and RNA sequencing suggesting an impairment in cytoskeleton and organization processes, we hypothesized that miR-155OE organoids would display aberrant organisation of the epithelial stratification process that is normally observed histology compared to control (Figure 5A). qRT-PCR of the primary esophageal tight junction molecules showed a significant decrease in the expression of *OCLN* (0.98 ± 0.01 vs 0.39 ± 0.16, Control vs miR-155OE, p≤0,05) and *CLDN7* (0.94 ± 0.01 vs 0.49 ± 0.04, Control vs miR-155OE, p≤0.001) (Figure 5B). We confirmed this by western blot showing a significant decrease in the expression of claudin-7 protein (3.05 ± 0.66 vs 1.02 ± 0.28, Control vs miR-155OE, p≤0.05) (Figure 5C). Owing to this decrease in claudin-7 mRNA and protein, histological staining was performed on FFPE miR-155OE organoids. H&E analysis of miR-155OE organoid architecture showed notable dilated intracellular spaces, phenocopying EoE patients localised at the basal organoid region which we did not observe

in the control organoids (Figure 5D). Furthermore, claudin-7 staining showed a standard membranous pattern within the control organoids, however claudin-7 was notably aberrant in the miR-155OE organoids whereby distinctly less membranous claudin-7 was observed which correlated with areas showing dilated intracellular spaces (Figure 5D). Owing to this indirect attenuation of claudin-7 by miR-155 overexpression, H&E analysis of claudin-7 knockdown (previously described[9]) organoids displayed perturbed histology and cellular dilations which were not observed in control organoids (Figure 5E), and which showed similarity to the dilated spaces observed in miR-155OE organoids phenocopying histological features associated with the EoE pathology.

Discussion

MiRNAs possess fundamental roles in both physiologic and pathologic processes including proliferation, differentiation, apoptosis, and regulation of inflammation. In this study we demonstrate that miR-155 is elevated in epithelia of active EoE patients and leads to functionally deficient esophageal epithelial barrier *in vitro*. We show that biopsies from active EoE patients display elevated epithelial miR-155 compared to uninflamed controls, and inactive EoE patients. Esophageal epithelial cells cultured in organotypic 3D-ALI display highest miR-155 in immature epithelial culture timepoints. Following recapitulation of the pathologic inflammatory hypoxic EoE microenvironment, we demonstrate that esophageal epithelial cells increase the expression of miR-155 during extended experimental hypoxia, inverse to its target *HIF1A* expression which we have shown previously to directly regulate claudin-1 expression in EoE[29]. Notably, we demonstrate that stable overexpression of miR-155 induces a dysfunctional esophageal epithelial barrier, which we confirm to be in part through the attenuation of the tight junction molecule claudin-7. Herein we suggest that the elevation of epithelial miR-155 induces a functionally deficient epithelial barrier and contributes to overall pathological esophageal epithelial dysfunction in EoE.

MiRNAs have previously been explored in EoE and shown to play key roles in the pathophysiology, such as correlating with eosinophilia and promoting the characteristic type-2 immune response[11–15]. Our data shows that miR-155 is elevated within the esophageal epithelium of EoE patients and resolves following successful treatment. A previous study which examined the differential expression of miRNAs in the mucosa of EoE patients using unbiased microarray approach showed that miR-155 is amongst those elevated in the esophageal epithelium and resolves post-treatment, however cellular source, localisation and functional consequence of miR-155 had yet to be explored[13]. Our data builds upon this by confirming that miR-155 is significantly elevated in esophageal tissues of EoE patients, is predominantly expressed in the basal and suprabasal layers of the esophageal epithelium, and resolves following successful treatment. This is in line with research that has shown the expression of miR-155 is elevated in $CD4^+$ T-cells from patients with an allergy to dust mite extract and which had either allergic rhinitis or asthma. MiR-155 expression was highest in $CD4^+$ T-cells from patients with asthma compared to allergic rhinitis and non-asthmatics and reduced following glucocorticoid treatment. However, the inhibitory effects of glucocorticoids on miR-155 was lost in patients with severe asthma[42]. Our data is concordant with this research in showing that miR-155 is elevated in patients with EoE and resolves following therapeutic intervention. The localisation of miR-155

predominantly in the basal region of esophageal biopsies of EoE patients mirrors our organotypic heterogenous 3D-ALI cultures whereby miR-155 is elevated in immature esophageal epithelial cells. The expression of miR-155 is inversely related to a selection of its targets, *CLDN1, TJP1, OCLN,* and *PTEN*, as well as that organoid cultures further display the action of miR-155 on tight junction expression and dilated epithelial spaces. Thus, we show that when we use heterocellular models such as 3D-ALI or organoid cultures which are more physiologically relevant than monolayer cultures the true impact of miR-155 can be elucidated in its role in driving epithelial barrier dysfunction. In a translational study using a mouse model of atopic dermatitis, authors showed by fluorescent *in situ* hybridisation that miR-155 was localised predominantly to epidermal keratinocytes and contributed to epithelial barrier loss through attenuation of a PKI-α/Claudin-1 axis[24]. The elevation in miR-155 was also observed in an *in vitro* model of psoriasis, whereby authors showed miR-155 expression was correlated with elevated IL-17 and IFNγ, as well as contributing to impaired barrier in skin keratinocytes[22]. Our findings contribute to a new and growing body of literature to support the concept that miR-155 is not a restrictively a leukocytic microRNA, and indeed it is increasingly evident that this microRNA may play an important role in regulating multiple epithelial barriers via the regulation of tight junction molecules[22,24,27,43–45].

MiR-155 has been associated with the progression of type-2 inflammatory processes in human and preclinical models of allergic rhinitis, asthma, and atopic dermatitis which can present as comorbid atopies in patients with EoE[19–21,24,28,46]. Research in mouse models of allergic asthma demonstrated a previously unknown role of miR-155 in the promotion of type-2 inflammation. Ovalbumin (OVA) challenged miR-155KO (knock out) mice showed impaired type-2 cytokine (IL-4, IL-5, IL-13) production, reduced mucus secretion, and attenuated eosinophil infiltration in the lungs of challenged mice[20]. Subsequent studies defined miR-155 as a positive regulator of allergen-induced inflammation via type 2 innate lymphoid cells (ILC2s) and IL-33[19]. Studies investigating atopic dermatitis also show an elevation in miR-155 in mouse models[24] and patients[28,47]. Collectively, these studies identified miR-155 as a key mediator in the progression of type-2 allergic inflammation and contribute to epithelial dysfunction.

As we have demonstrated previously, invading eosinophils and leukocytes such as that characteristic of the type-2 immune response in EoE sequester available oxygen in the esophageal epithelium and create a pathologically hypoxic microenvironment[29]. Mucosal surfaces are unique in that they border the external environment and possess dynamic physiological oxygen requirements (physioxia). We have previously shown that physioxia in the EoE esophagus is perturbed towards a pathological hypoxic microenvironment, contributed in part by invading eosinophil oxygen consumption. We showed that in contrast to acute hypoxic exposures, chronicity of inflammatory hypoxia leads to a maladaptive response in the esophageal epithelium which impairs HIF-1α signaling and dysregulates the HIF-1α regulated tight junction claudin-1 contributing to epithelial barrier dysfunction[29]. Interestingly, we showed an exclusive regulation of Claudin-1 by hypoxia, but not its esophageal tight junction counterparts Claudins 4 or 7. Our own and research published by others have elucidated that all three esophageal tight junction claudins, 1, 4 and 7 are decreased in patients with EoE, via multiple and varied mechanism's including via

inflammatory cytokines TGF-b1 and IL-9.[9,29,31,32] The studies within, expand upon those inflammatory regulators to now consider microRNA mediated regulation of these junctional components, also suggesting that while hypoxia/HIF does not directly regulate Claudin 7, it may do so via hypoxia mediated induction of miR-155.

The alteration in mucosal oxygen towards pathological hypoxia and its impact on miRNA and HIF alpha isoform expression has been suggested previously[48]. Notably, the elevation of miR-155 in extended experimental hypoxia was shown in intestinal colon cancer cell lines[25]. Authors showed using unbiased microarray analysis that miR-155 was among several miRNAs that were elevated in intestinal Caco-2 cells cultured in extended experimental hypoxia. This elevation in miR-155 was inverse to HIF-1α signaling and contributed to the destabilisation of *HIF1A* in hypoxic cancer cells and mouse tissue. Neutralisation of endogenous miR-155 reversed the inhibition of HIF-1α activity, and validated miR-155- as a key player of the isoform-specific HIF-1α negative-feedback loop. Previous studies have also confirmed the importance of HIF-1α regulation in epithelial barrier[18,49]. The miR-155/HIF-1α regulatory axis has previously shown to contribute to barrier dysfunction at the mucosa in dextran sulfate sodium (DSS) induced colitis. Authors showed that DSS treated mice had markedly elevated miR-155 and confirmed via dual luciferase reporter assay that miR-155 interacted with and destabilised HIF-1α. This inverse relationship contributed to impaired barrier via attenuation of the HIF-1α/TFF-3 axis in colonic epithelia, which was reversed following miR-155 antagomir treatment[18]. Herein our data validates miR-155 as a hypoxia-responsive miRNA of the esophageal epithelium and supports its action within the regulation of overall HIF-1α signalling. These data may contribute to future studies investigating the therapeutic utility of miRNAs in restoring functional epithelial barrier regarding the pathologically hypoxic EoE microenvironment.

Independent of the complexities associated with experimental hypoxia, it is demonstrated herein that miR-155 overexpression induced a dysfunctional epithelial barrier in esophageal epithelial cells. As described previously miR-155 expression contributed to epithelial barrier dysfunction through tight junction regulation in skin, bronchial, and intestinal epithelia[22,24,27,43–45]. Tight junction protein claudin-1 has been shown as a miR-155 target in epithelial tissue[45], the loss of which induces epithelial dysfunction in different diseases[27,29,49]. A previous study using mouse models showed that the overexpression of miR-155 dysregulates intestinal epithelial barrier associated with severe acute pancreatitis. This increase in miR-155 inhibited ZO-1 and E-Cadherin through the attenuation of RhoA[43]. However, the impact of miR-155 overexpression on esophageal epithelial cell function has not yet been explored. Comparative analysis between RNA sequencing of miR-155OE cells cultured in 3D-ALI and a publicly available transcriptomic dataset showed an overlap in 167 genes of which there was enrichment for the cornified envelope, desmosome, intermediate filament and keratin filament which have previously been shown in the context of EoE pathogenesis[40]. We show for the first time that miR-155 overexpression induces a dysfunctional barrier in esophageal epithelial cells cultured in physiologic 3D-ALI and organoid cultures, and that miR-155 elevation also regulates tight junction expression by attenuation of claudin-7.

Claudins are transmembrane proteins that are expressed in a variety of tissues and possess a dual function within epithelia. There exist barrier-forming claudins which maintain tight epithelial barrier between adjacent epithelial cells, and pore-forming claudins that increase tissue permeability[50]. We have shown previously that an attenuation of caudin-7 is associated with dysfunctional epithelial barrier and contributes to the pathophysiology consistent with EoE disease[9]. Our work showed the increase in EoE-associated TGF-β1 promoted esophageal epithelial barrier dysfunction through the attenuation of claudin-7. Additionally, claudin-7 knockdown esophageal epithelial cells displayed impaired epithelial barrier as measured by TEER and FITC dextran paracellular flux (FITC flux). Notably here, our data shows that the overexpression of miR-155 is associated with epithelial barrier impairment which we have confirmed by TEER in physiologically relevant 3D-ALI cultures, as well as showing that barrier impairment in miR-155OE cells is governed by an attenuation in claudin-7 both at the mRNA and protein expression level. We also show the attenuation in tight junction regulation, including claudin-7 in miR-155OE esophageal epithelial organoids. It is evident that there are alterations in the localisation of claudin-7, which we found to correlate with dilated intracellular spaces and contribute to overall attenuation in esophageal epithelial barrier. Visual comparisons between organoid histology in miR-155OE and claudin-7KD organoids showed similarity in epithelial dilations and overall perturbed histology compared to relevant controls. The perimembranous expression of claudin-7 observed in our miR-155OE cells is reminiscent of that seen in patient biopsies in our previous studies[9]. Moreover, we show that RNA sequencing of miR-155OE cells contribute to our understanding of epithelial barrier breakdown by showing an overlap in gene signatures that have previously been shown as candidate transcripts in the molecular analysis of EoE[51]. Usage of online databases of miR-155 targets and manual curation of the 3'UTR and 5'UTR of claudin-7 mRNA and found no complementarity to which the miR-155 seed region could bind, thus showing that miR-155 overexpression is indirectly associated with claudin-7 attenuation. Analysis of the claudin-7 promoter using UCSC genome browser[52] and JASPAR[53] identified putative binding sites for transcription factors HNF4α and PU.1. A key role for HNF4α and PU.1 in regulating *CLDN7* expression in intestinal epithelial cells has previously been identified, confirming via chromatin immunoprecipitation a direct regulation of *CLDN7* by HNF4α[54]. *In silico* analysis of these transcription factors identifies them as predicted miR-155 targets (Figure 5F), however their differential regulation in the context of EoE has yet to be fully explored. Our data contributes to our collective and wider understanding on the action of epithelial miR-155 in promoting a dysfunctional epithelial barrier through a yet unknown attenuation of claudin-7.

Limitations do exist within our study. Our experiments do not include the addition of multicellular systems or *in vivo* models due to the reductionist approach we undertook to investigate the novel and previously unstudied specific epithelial defects associated with the elevation of miR-155. In this regard, future studies should elucidate the role of this miRNA in other cells involved in the pathophysiology of EoE. However, given the pathological roles associated with miR-155 as previously described in other cell types, diseases, and models, it remains encouraging that future therapeutic targeting of miR-155 may have a multicellular beneficial effect.

In summary, our findings indicate that miR-155 in not solely a leukocytic miRNA but is shown to be produced within the esophageal epithelium and elevated in EoE. MiR-155 is a hypoxia responsive miRNA that is expressed during extended experimental hypoxia and displays an inverse relationship to HIF-1α. Stable overexpression of miR-155 leads to perturbations in epithelial barrier function, through indirect attenuation of tight junction claudin-7 expression. With reference to the growing body of literature that implicates epithelial barrier function in EoE pathophysiology, as well as in overall comorbid atopies, our findings contribute to the role of miR-155 in potentiating loss epithelial integrity in EoE. The overexpression of miR-155 plays a key role in diminishing epithelial barrier and creates an attractive opportunity for the utility of miRNAs in general as therapeutic targets in the restoration of the dysfunctional epithelial barrier in eosinophilic esophagitis.

Acknowledgements

The authors wish to thank the members of the participating laboratories for insightful discussions and critical comments. We thank the physicians, nurses, research assistants, pathology staff and endoscopy technical staff at Children's Hospital Colorado who contributed to this work by helping to provide and collect samples and recruit subjects. We are grateful to the patients and families who consented to be a part of this study.

Funding Support

This publication has emanated from research conducted with the financial support of Science Foundation Ireland under Grant numbers 17/FRL/4863 (JCM) and 18/FRL/6201 (EMcN), and from the NIH NIDDK under grant number K23DK109263 (CMK). Support (GTF) from LaCache Chair in Gastrointestinal Allergic and Immunological Diseases, Children's Hospital Colorado. GEM was supported by a Maynooth University Kathleen Lonsdale Institute for Human Health Research PhD scholarship scheme grant awarded to JCM.

Role of the Funding Source

The study sponsors played no role in the study design in the collection, analysis, and interpretation of data or preparation of this article. Manuscript contents are the authors' sole responsibility and do not necessarily represent official NIH views.

Data sharing statement

The data that support the findings of this study are available on request from the corresponding author. The RNASeq data discussed in this publication are accessible through GEO Series accession number GSE197702 and GSE244629

Bibliography

1. Dellon ES, Liacouras CA, Molina-Infante J, et al. Updated International Consensus Diagnostic Criteria for Eosinophilic Esophagitis: Proceedings of the AGREE Conference. Gastroenterology. Oct 2018;155(4):1022–1033.e10. doi:10.1053/j.gastro.2018.07.009 [PubMed: 30009819]
2. Collins MH. Histopathology of eosinophilic esophagitis. Dig Dis. 2014;32(1–2):68–73. doi:10.1159/000357012 [PubMed: 24603383]
3. Clevenger MH, Karami AL, Carlson DA, et al. Suprabasal cells retain progenitor cell identity programs in eosinophilic esophagitis-driven basal cell hyperplasia. JCI Insight. Sep 5 2023;doi:10.1172/jci.insight.171765
4. Blanchard C, Stucke EM, Burwinkel K, et al. Coordinate Interaction between IL-13 and Epithelial Differentiation Cluster Genes in Eosinophilic Esophagitis. The Journal of Immunology. 2010;184(7):4033–4041. doi:10.4049/jimmunol.0903069 [PubMed: 20208004]

5. Kottyan LC, Davis BP, Sherrill JD, et al. Genome-wide association analysis of eosinophilic esophagitis provides insight into the tissue specificity of this allergic disease. Nature Genetics. 2014;46(8):895–900. doi:10.1038/ng.3033 [PubMed: 25017104]
6. Zeng C, Vanoni S, Wu D, et al. Solute carrier family 9, subfamily A, member 3 (SLC9A3)/sodium-hydrogen exchanger member 3 (NHE3) dysregulation and dilated intercellular spaces in patients with eosinophilic esophagitis. J Allergy Clin Immunol. Dec 2018;142(6):1843–1855. doi:10.1016/j.jaci.2018.03.017 [PubMed: 29729938]
7. Rochman M, Azouz NP, Rothenberg ME. Epithelial origin of eosinophilic esophagitis. J Allergy Clin Immunol. Jul 2018;142(1):10–23. doi:10.1016/j.jaci.2018.05.008 [PubMed: 29980278]
8. Capocelli KE, Fernando SD, Menard-Katcher C, Furuta GT, Masterson JC, Wartchow EP. Ultrastructural features of eosinophilic oesophagitis: Impact of treatment on desmosomes. Journal of Clinical Pathology. 2015;68(1):51–56. doi:10.1136/jclinpath-2014-202586 [PubMed: 25359789]
9. Nguyen N, Fernando SD, Biette KA, et al. TGF-β1 alters esophageal epithelial barrier function by attenuation of claudin-7 in eosinophilic esophagitis. Mucosal Immunol. Mar 2018;11(2):415–426. doi:10.1038/mi.2017.72 [PubMed: 28832026]
10. Markey GE, Donohoe CL, McNamee EN, Masterson JC. MicroRNA dysregulation and therapeutic opportunities in esophageal diseases. Am J Physiol Gastrointest Liver Physiol. Jul 1 2023;325(1):G1–g13. doi:10.1152/ajpgi.00184.2022 [PubMed: 37129237]
11. Zahm AM, Menard-Katcher C, Benitez AJ, et al. Pediatric eosinophilic esophagitis is associated with changes in esophageal microRNAs. American Journal of Physiology - Gastrointestinal and Liver Physiology. 2014;307(8):G803–G812. doi:10.1152/ajpgi.00121.2014 [PubMed: 25147232]
12. Lu TX, Sherrill JD, Wen T, et al. MicroRNA signature in patients with eosinophilic esophagitis, reversibility with glucocorticoids, and assessment as disease biomarkers. Journal of Allergy and Clinical Immunology. 2012;129(4):1064–75.e9. doi:10.1016/j.jaci.2012.01.060 [PubMed: 22391115]
13. Lu S, Mukkada VA, Mangray S, et al. MicroRNA profiling in mucosal biopsies of eosinophilic esophagitis patients pre and post treatment with steroids and relationship with mRNA targets. PLoS ONE. 2012;7(7)doi:10.1371/journal.pone.0040676
14. Cañas JA, Tabares A, Barbero C, et al. Proton-pump Inhibitor Response Prediction Using Esophageal microRNAs in Children With Eosinophilic Esophagitis. Journal of pediatric gastroenterology and nutrition. 2020;71(6):755–763. doi:10.1097/MPG.0000000000002957 [PubMed: 33003164]
15. Lu TX, Rothenberg ME. Diagnostic, functional, and therapeutic roles of microRNA in allergic diseases. The Journal of allergy and clinical immunology. 2013;132(1):3–14. doi:10.1016/j.jaci.2013.04.039 [PubMed: 23735656]
16. Eis PS, Tam W, Sun L, et al. Accumulation of miR-155 and BIC RNA in human B cell lymphomas. Proceedings of the National Academy of Sciences of the United States of America. 2005;102(10):3627–3632. doi:10.1073/pnas.0500613102 [PubMed: 15738415]
17. Zhou H, Huang X, Cui H, et al. MiR-155 and its star-form partner miR-155* cooperatively regulate type I interferon production by human plasmacytoid dendritic cells. Blood. 2010;116(26):5885–5894. doi:10.1182/blood-2010-04-280156 [PubMed: 20852130]
18. Liu Y, Zhu F, Li H, et al. MiR-155 contributes to intestinal barrier dysfunction in DSS-induced mice colitis via targeting HIF-1α/TFF-3 axis. Aging (Albany NY). Jul 26 2020;12(14):14966–14977. doi:10.18632/aging.103555 [PubMed: 32713852]
19. Johansson K, Malmhäll C, Ramos-Ramírez P, Rådinger M. MicroRNA-155 is a critical regulator of type 2 innate lymphoid cells and IL-33 signaling in experimental models of allergic airway inflammation. The Journal of Allergy and Clinical Immunology. 2017;139(3):1007–1016.e9. doi:10.1016/j.jaci.2016.06.035 [PubMed: 27492144]
20. Malmhäll C, Alawieh S, Lu Y, et al. MicroRNA-155 is essential for T(H)2-mediated allergen-induced eosinophilic inflammation in the lung. The Journal of Allergy and Clinical Immunology. 2014;133(5):1429–1438, 1438.e1–7. doi:10.1016/j.jaci.2013.11.008 [PubMed: 24373357]
21. Suojalehto H, Toskala E, Kilpeläinen M, et al. MicroRNA profiles in nasal mucosa of patients with allergic and nonallergic rhinitis and asthma. International Forum of Allergy & Rhinology. 2013;3(8):612–620. doi:10.1002/alr.21179 [PubMed: 23704072]

22. Beer L, Kalinina P, Köcher M, et al. miR-155 Contributes to Normal Keratinocyte Differentiation and Is Upregulated in the Epidermis of Psoriatic Skin Lesions. Int J Mol Sci. Dec 5 2020;21(23)doi:10.3390/ijms21239288
23. Xu L, Leng H, Shi X, Ji J, Fu J, Leng H. MiR-155 promotes cell proliferation and inhibits apoptosis by PTEN signaling pathway in the psoriasis. Biomed Pharmacother. Jun 2017;90:524–530. doi:10.1016/j.biopha.2017.03.105 [PubMed: 28402921]
24. Wang X, Chen Y, Yuan W, et al. MicroRNA-155–5p is a key regulator of allergic inflammation, modulating the epithelial barrier by targeting PKIα. Cell Death & Disease. 2019;10(12)doi:10.1038/s41419-019-2124-x
25. Bruning U, Cerone L, Neufeld Z, et al. MicroRNA-155 promotes resolution of hypoxia-inducible factor 1alpha activity during prolonged hypoxia. Mol Cell Biol. Oct 2011;31(19):4087–96. doi:10.1128/mcb.01276-10 [PubMed: 21807897]
26. Yao M, Wang X, Tang Y, et al. Dicer mediating the expression of miR-143 and miR-155 regulates hexokinase II associated cellular response to hypoxia. Am J Physiol Lung Cell Mol Physiol. Dec 1 2014;307(11):L829–37. doi:10.1152/ajplung.00081.2014 [PubMed: 25172909]
27. Hiranuma H, Gon Y, Maruoka S, et al. DsRNA induction of microRNA-155 disrupt tight junction barrier by modulating claudins. Asia Pacific Allergy. 2020;10(2)doi:10.5415/apallergy.2020.10.e20
28. Sonkoly E, Janson P, Majuri M-L, et al. MiR-155 is overexpressed in patients with atopic dermatitis and modulates T-cell proliferative responses by targeting cytotoxic T lymphocyte-associated antigen 4. The Journal of Allergy and Clinical Immunology. 2010;126(3):520–581. doi:10.1016/j.jaci.2010.05.045
29. Masterson JC, Biette KA, Hammer JA, et al. Epithelial HIF-1α/claudin-1 axis regulates barrier dysfunction in eosinophilic esophagitis. The Journal of Clinical Investigation. 2019;129(8):3224–3235. doi:10.1172/JCI126744 [PubMed: 31264974]
30. Katzka DA, Tadi R, Smyrk TC, et al. Effects of topical steroids on tight junction proteins and spongiosis in esophageal epithelia of patients with eosinophilic esophagitis. Clin Gastroenterol Hepatol. Nov 2014;12(11):1824–9 e1. doi:10.1016/j.cgh.2014.02.039 [PubMed: 24681080]
31. Ruffner MA, Song L, Maurer K, et al. Toll-like receptor 2 stimulation augments esophageal barrier integrity. Allergy. Dec 2019;74(12):2449–2460. doi:10.1111/all.13968 [PubMed: 31267532]
32. Doshi A, Khamishon R, Rawson R, et al. Interleukin 9 Alters Epithelial Barrier and E-cadherin in Eosinophilic Esophagitis. J Pediatr Gastroenterol Nutr. Feb 2019;68(2):225–231. doi:10.1097/mpg.0000000000002144 [PubMed: 30211842]
33. Wu L, Oshima T, Li M, et al. Filaggrin and tight junction proteins are crucial for IL-13-mediated esophageal barrier dysfunction. Am J Physiol Gastrointest Liver Physiol. Sep 1 2018;315(3):G341–g350. doi:10.1152/ajpgi.00404.2017 [PubMed: 29746170]
34. Sherrill JD, Kc K, Wu D, et al. Desmoglein-1 regulates esophageal epithelial barrier function and immune responses in eosinophilic esophagitis. Mucosal Immunology. 2014;7(3):718–729. doi:10.1038/mi.2013.90 [PubMed: 24220297]
35. Hara T, Kasagi Y, Wang J, et al. CD73(+) Epithelial Progenitor Cells That Contribute to Homeostasis and Renewal Are Depleted in Eosinophilic Esophagitis. Cell Mol Gastroenterol Hepatol. 2022;13(5):1449–1467. doi:10.1016/j.jcmgh.2022.01.018 [PubMed: 35108658]
36. McGeary SE, Lin KS, Shi CY, et al. The biochemical basis of microRNA targeting efficacy. Science. Dec 20 2019;366(6472)doi:10.1126/science.aav1741
37. Huang HY, Lin YC, Cui S, et al. miRTarBase update 2022: an informative resource for experimentally validated miRNA-target interactions. Nucleic Acids Res. Jan 7 2022;50(D1):D222–d230. doi:10.1093/nar/gkab1079 [PubMed: 34850920]
38. Garcia E, Ladak Z, Landry T, et al. Epithelial-mesenchymal transition, regulated by β-catenin and Twist, leads to esophageal wall remodeling in pediatric eosinophilic esophagitis. PLoS One. 2022;17(3):e0264622. doi:10.1371/journal.pone.0264622 [PubMed: 35239721]
39. Azouz NP, Ynga-Durand MA, Caldwell JM, et al. The antiprotease SPINK7 serves as an inhibitory checkpoint for esophageal epithelial inflammatory responses. Sci Transl Med. Jun 6 2018;10(444)doi:10.1126/scitranslmed.aap9736

40. Kc K, Rothenberg ME, Sherrill JD. In vitro model for studying esophageal epithelial differentiation and allergic inflammatory responses identifies keratin involvement in eosinophilic esophagitis. PLoS One. 2015;10(6):e0127755. doi:10.1371/journal.pone.0127755 [PubMed: 26039063]
41. Menard-Katcher C, Liu C, Galbraith MD, et al. Fibrostenotic eosinophilic esophagitis phenotype is defined by a proliferative gene signature. Allergy. Feb 2023;78(2):579–583. doi:10.1111/all.15557 [PubMed: 36273270]
42. Daniel E, Roff A, Hsu MH, Panganiban R, Lambert K, Ishmael F. Effects of allergic stimulation and glucocorticoids on miR-155 in CD4(+) T-cells. Am J Clin Exp Immunol. 2018;7(4):57–66. [PubMed: 30245919]
43. Tian R, Wang RL, Xie H, Jin W, Yu KL. Overexpressed miRNA-155 dysregulates intestinal epithelial apical junctional complex in severe acute pancreatitis. World J Gastroenterol. Dec 7 2013;19(45):8282–91. doi:10.3748/wjg.v19.i45.8282 [PubMed: 24363519]
44. Zhao X, Zeng H, Lei L, et al. Tight junctions and their regulation by non-coding RNAs. Int J Biol Sci. 2021;17(3):712–727. doi:10.7150/ijbs.45885 [PubMed: 33767583]
45. Zhang GJ, Xiao HX, Tian HP, Liu ZL, Xia SS, Zhou T. Upregulation of microRNA-155 promotes the migration and invasion of colorectal cancer cells through the regulation of claudin-1 expression. Int J Mol Med. Jun 2013;31(6):1375–80. doi:10.3892/ijmm.2013.1348 [PubMed: 23588589]
46. Okoye IS, Czieso S, Ktistaki E, et al. Transcriptomics identified a critical role for Th2 cell-intrinsic miR-155 in mediating allergy and antihelminth immunity. Proceedings of the National Academy of Sciences of the United States of America. 2014;111(30):E3081–E3090. doi:10.1073/pnas.1406322111 [PubMed: 25024218]
47. Sonkoly E, Ståhle M, Pivarcsi A. MicroRNAs: novel regulators in skin inflammation. Clin Exp Dermatol. May 2008;33(3):312–5. doi:10.1111/j.1365-2230.2008.02804.x [PubMed: 18419608]
48. Serocki M, Bartoszewska S, Janaszak-Jasiecka A, Ochocka RJ, Collawn JF, Bartoszewski R. miRNAs regulate the HIF switch during hypoxia: a novel therapeutic target. Angiogenesis. May 2018;21(2):183–202. doi:10.1007/s10456-018-9600-2 [PubMed: 29383635]
49. Saeedi BJ, Kao DJ, Kitzenberg DA, et al. HIF-dependent regulation of claudin-1 is central to intestinal epithelial tight junction integrity. Mol Biol Cell. Jun 15 2015;26(12):2252–62. doi:10.1091/mbc.E14-07-1194 [PubMed: 25904334]
50. Gunzel D, Yu AS. Claudins and the modulation of tight junction permeability. Physiol Rev. Apr 2013;93(2):525–69. doi:10.1152/physrev.00019.2012 [PubMed: 23589827]
51. Wen T, Stucke EM, Grotjan TM, et al. Molecular diagnosis of eosinophilic esophagitis by gene expression profiling. Gastroenterology. Dec 2013;145(6):1289–99. doi:10.1053/j.gastro.2013.08.046 [PubMed: 23978633]
52. Kent WJ, Sugnet CW, Furey TS, et al. The human genome browser at UCSC. Genome Res. Jun 2002;12(6):996–1006. doi:10.1101/gr.229102 [PubMed: 12045153]
53. Castro-Mondragon JA, Riudavets-Puig R, Rauluseviciute I, et al. JASPAR 2022: the 9th release of the open-access database of transcription factor binding profiles. Nucleic Acids Res. Jan 7 2022;50(D1):D165–d173. doi:10.1093/nar/gkab1113 [PubMed: 34850907]
54. Farkas AE, Hilgarth RS, Capaldo CT, et al. HNF4α regulates claudin-7 protein expression during intestinal epithelial differentiation. Am J Pathol. Aug 2015;185(8):2206–18. doi:10.1016/j.ajpath.2015.04.023 [PubMed: 26216285]

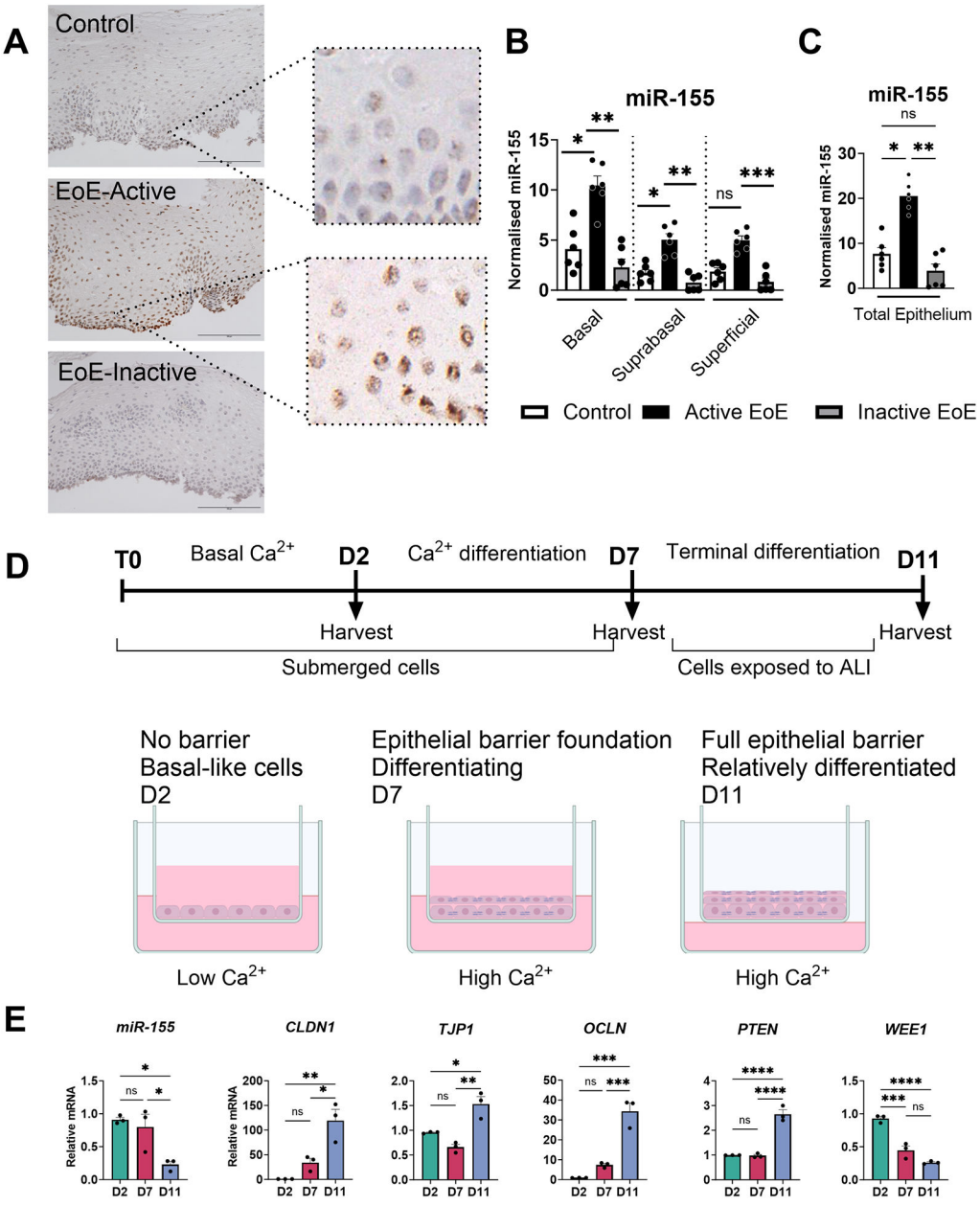

Figure 1: Epithelial miR-155 is elevated in active EoE and is highest in immature esophageal epithelial cells at 3D-ALI.

(A) Representative images of miR-155 in *situ* hybridisation on biopsies from uninflamed controls, active EoE, and inactive EoE. (B) Compartmental analysis on the individual esophageal layers shows that miR-155 was highest within the basal and suprabasal regions in active EoE and further reduced through therapeutic intervention in inactive EoE. (C) Total epithelial miR-155 was also evaluated by merging the data of the three constituent esophageal layers and found that EoE patients display significantly higher miR-155 than uninflamed controls and inactive EoE individuals. (D) EPC2-hTERTs were grown in organotypic 3D-ALI culture and harvested on day 2, 7 and 11. The expression of miR-155 was elevated during immature epithelial developmental timepoints on (E) days 2 and 7.

Predicted miR-155 targets *CLDN1, TJP1, OCLN,* and *PTEN* were investigated by qRT-PCR and found to display inverse kinetics to the expression of miR-155 at 3D-ALI. Statistical significance of ISH data was assessed using a Kruskal-Wallis test with a Dunn's multiple comparisons test. 3D-ALI data was assessed for significance using a One-Way ANOVA with a Tukey's multiple comparisons test. *P ≤ 0.05, **P ≤ 0.01, ***P ≤ 0.001. Data are presented as means ± SEM and represent 3 experimental repeats.

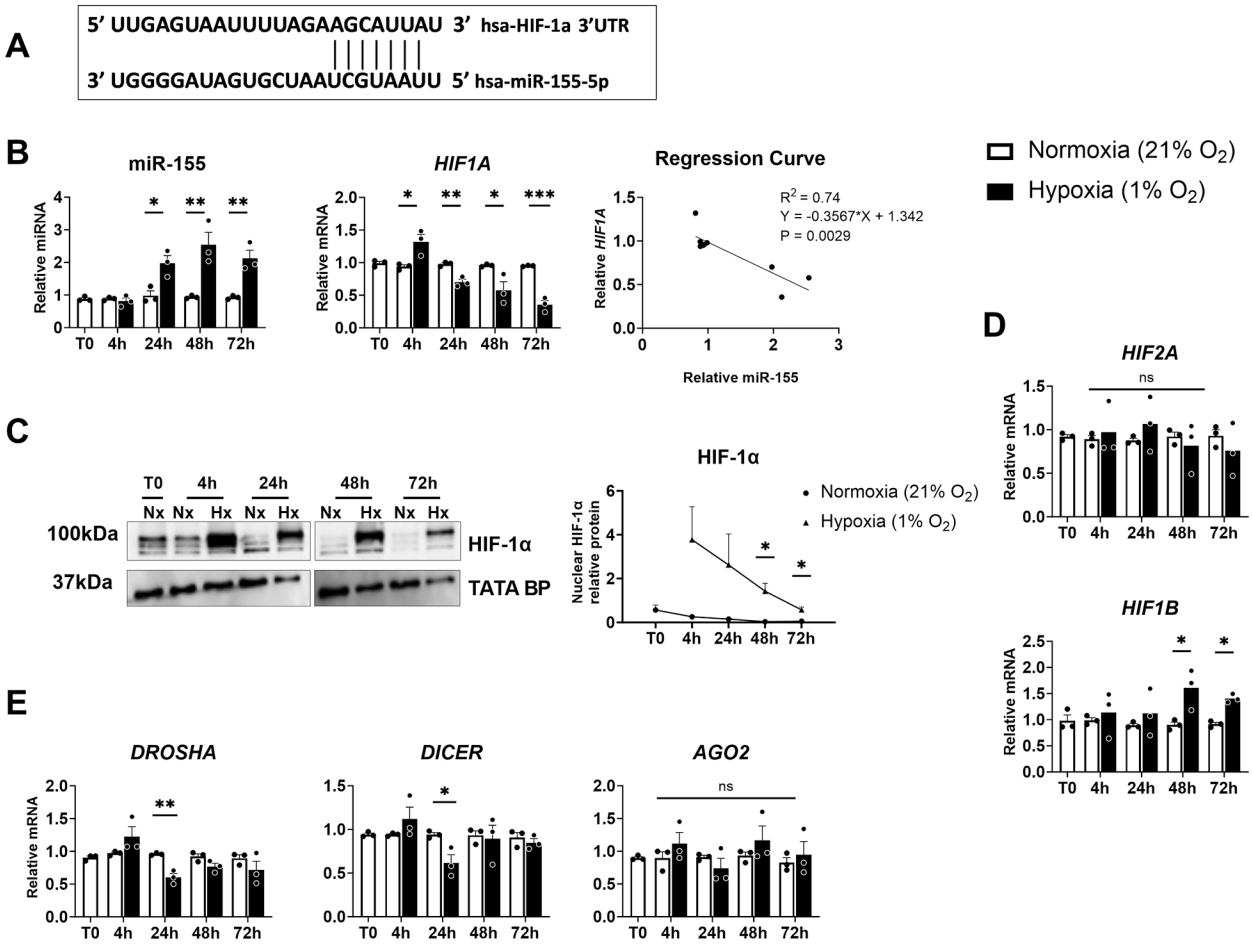

Figure 2: Extended experimental hypoxia induces miR-155 and differentially regulates its targets.

(A) Complimentary binding of the *HIF1A* 3' UTR to that of the miR-155 seed region. (B) *HIF1A* and miR-155 expression was assessed by qRT-PCR from esophageal epithelial cells exposed to a time course (0, 4, 24, 48, 72 hours) of experimental hypoxia compared with time matched normoxic controls. Inverse linear regression analysis was carried out to show the significantly inverse relationship between the expression of miR-155 and *HIF1A* in experimental hypoxia. (C) HIF-1α expression was assessed by Western blotting of nuclear isolates from esophageal epithelial cells exposed to a time course (0, 4, 24, 48, 72 hours) of experimental hypoxia compared to time matched normoxic controls. (D and E) qRT-PCR analysis of *HIF2A* and *HIF1B* (D), and miRNA processing genes *DROSHA, DICER, and AGO2* (E). For Western blots, a representative for a single time course are presented. Statistical significance was assessed using a Students' t test comparing time point–matched normoxic controls with hypoxic samples. *P < 0.05, **P < 0.01, ***P < 0.001 (n = 3). Data are presented as means ± SEM and represent 3 experimental repeats.

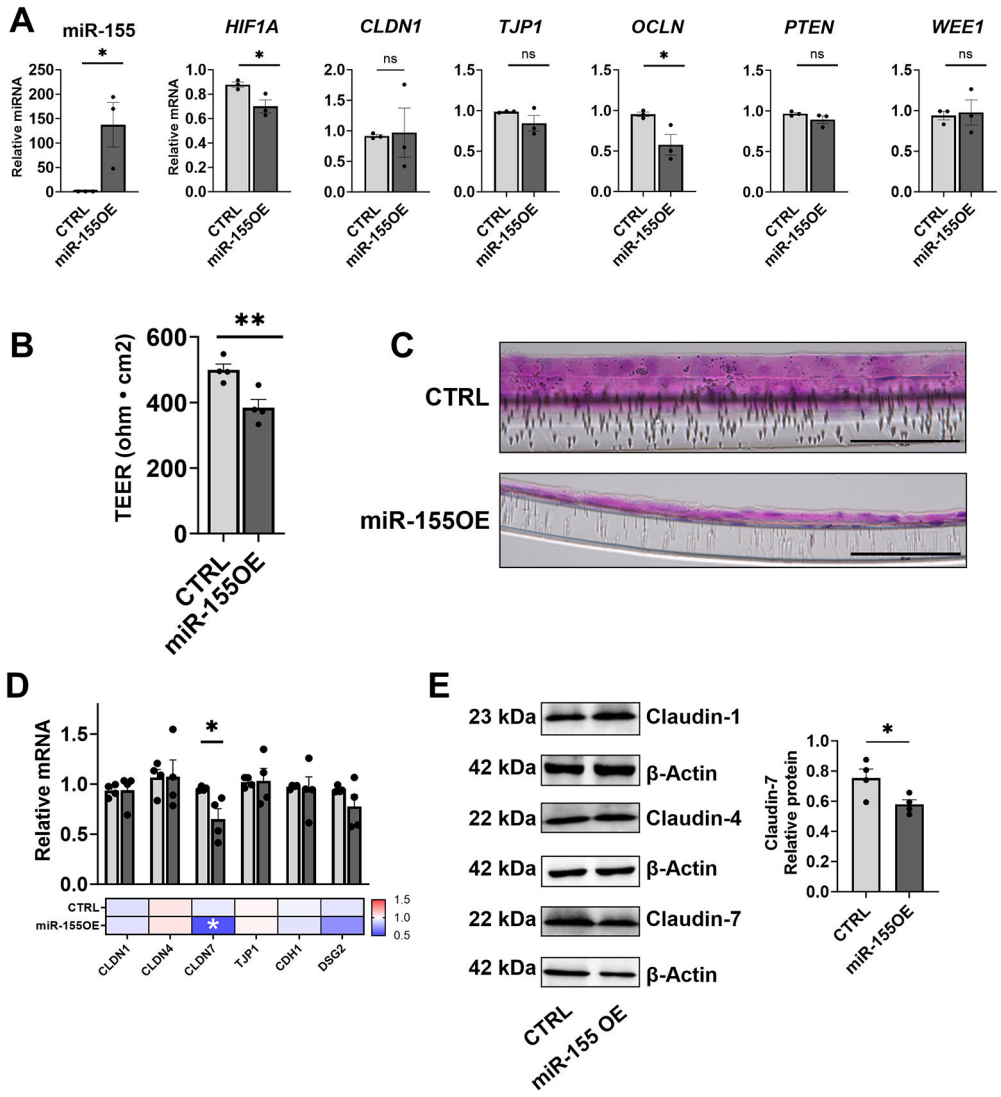

Relative protein expression (Actin)	miR-155OE Fold Change ± SEM	Significance
Claudin-1	1.3 ± 0.29	n.s.
Claudin-4	0.51 ± 0.14	n.s.
Claudin-7	0.58 ± 0.06	p≤0.05

Figure 3: Stable miR-155–5p overexpression reduces HIF-1α signaling and induces a deficient epithelial barrier.

(A) Submerged monolayer cultures of miR-155OE cells shows a significant elevation in miR-155. qRT-PCR of miR-155 targets showed and attenuation of *HIF1A* in miR-155OE cells, and a significant decrease in *OCLN*. We did not observe significant differential expression in the remaining targets *CLDN1, TJP1, PTEN,* or *WEE1* in submerged culture. (B) Using stratified squamous 3-dimensional air liquid interface (3D-ALI) cultures, miR-155 overexpression diminished barrier as measured by transepithelial electrical resistance (TEER) (n=4). (C) H&E stained sections from miR-155OE cells cultured at 3D-ALI indicate perturbed stratification. Black scale bar represents 60 μm. These data suggest that in the setting of miR-155OE, epithelial defects exist. (D) qRT-PCR of barrier-forming

molecules showed a significant decrease in the tight junction *CLDN7*. (E) Whole cell protein was analysed by Western blot whereby claudin-7 was shown to be attenuated in miR-155OE cells in 3D-ALI. Submerged culture data was analysed for significance using a Students' t test comparing time point–matched controls. *P < 0.05, **P < 0.01, ***P < 0.001. Data are presented as means ± SEM and represent a minimum of 3 experimental repeats.

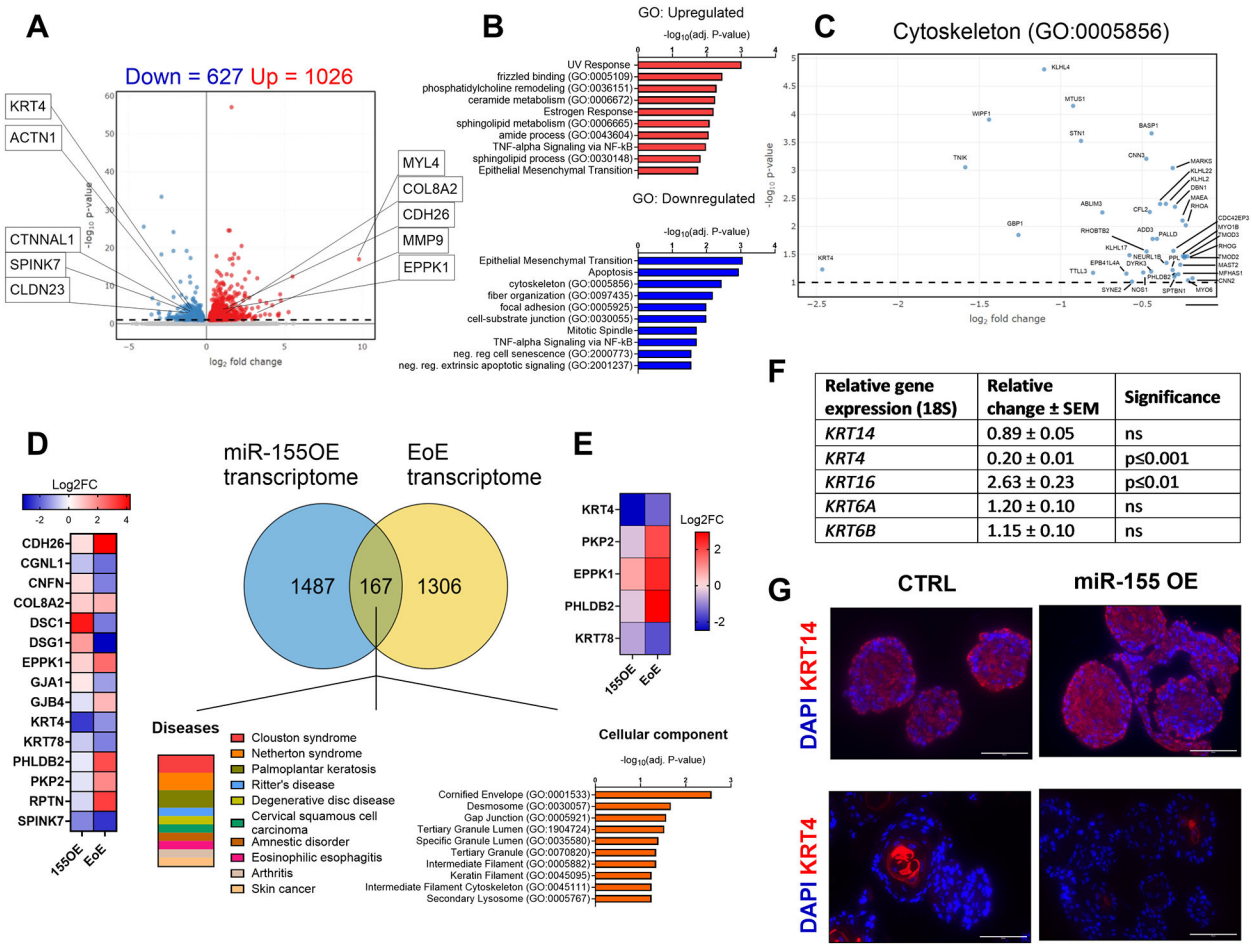

Relative gene expression (18S)	Relative change ± SEM	Significance
KRT14	0.89 ± 0.05	ns
KRT4	0.20 ± 0.01	p≤0.001
KRT16	2.63 ± 0.23	p≤0.01
KRT6A	1.20 ± 0.10	ns
KRT6B	1.15 ± 0.10	ns

Figure 4: MiR-155 overexpression dysregulates esophageal epithelial function.

RNA sequencing of miR-155OE and control cells cultured at 3D-ALI shows impaired epithelial function. (A) Significance was attributed to differentially expressed genes with an adjusted p-value ≤0.1. and yielded 627 downregulated genes and 1026 upregulated genes. A selection of genes were selected which have functions within cytoskeleton and epithelial organisation or have been validated in the literature to contribute to EoE pathophysiology. (B) GO analysis for pathway enrichment for upregulated and downregulated pathways in miR-155OE cells. (C) Venn diagram showing the number of genes differentially expressed as identified by publicly available RNA-seq of patients with inflammatory EoE as compared to controls (cut-off of fold change > 2 or < 0.5, adjusted p-value < 0.05) and in miR-155OE cells in 3D-ALI cultures for 11 days. Genes overlapping between these two data sets were identified (167 genes) and a selection with functions relevant to EoE pathophysiology were graphed into a heatmap. GO analyses of the miR-155OE-EoE overlap gene set depicted localization of cellular components and enrichment of diseases based on the 167 gene overlap based on adjusted p-value (-log10) showed a selection of diseases with perturbed epithelial function including Clouston syndrome, Netherton syndrome, Palmoplantar keratosis, and Eosinophilic esophagitis. GO analysis of the 167 intersected genes' enriched pathways involved 'intermediate filament', 'keratin filament', and 'intermediate filament cytoskeleton' which shared 5 genes. These pathways reveal

a dysregulation in cytoskeletal arrangement of miR-155OE cells. (D) Immunofluorescent stained miR-155OE organoids show no difference in basal KRT14, however miR-155OE organoids display less intense and mislocalized KRT4. (E) qRT-PCR of miR-155OE showing differential expression of an array of basal and suprabasal keratins.

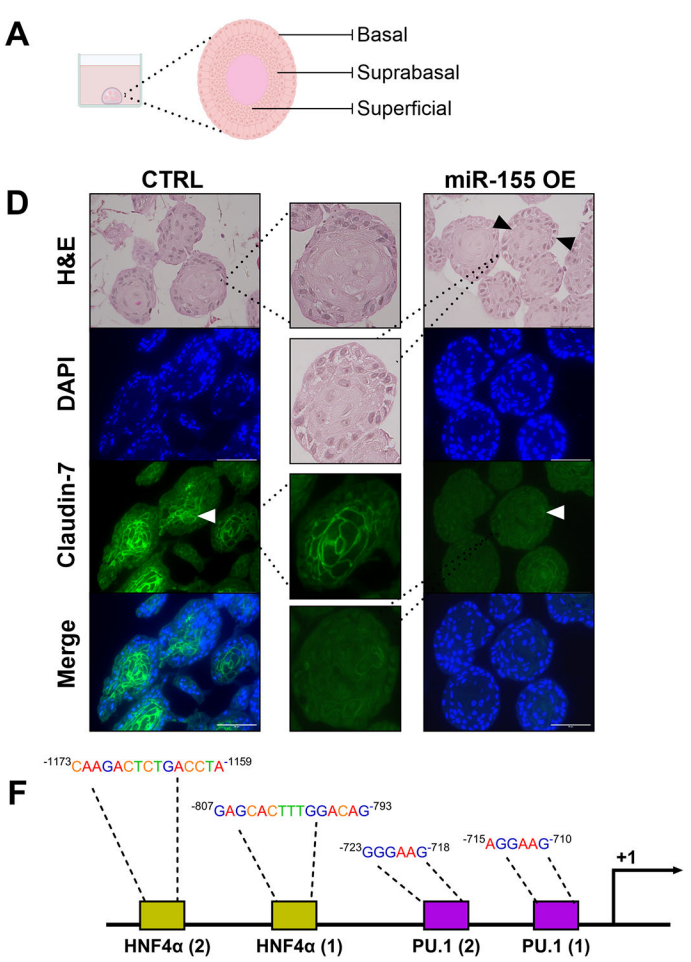

B

Relative gene expression (18S)	Relative change ± SEM	Significance
CLDN1	1.37 ± 0.20321	ns
CLDN4	0.65 ± 0.14	ns
CLDN7	0.5198 ± 0.04	p≤0.001
OCLN	0.40077 ± 0.16	p≤0.05
TJP1	0.85236 ± 0.13	ns

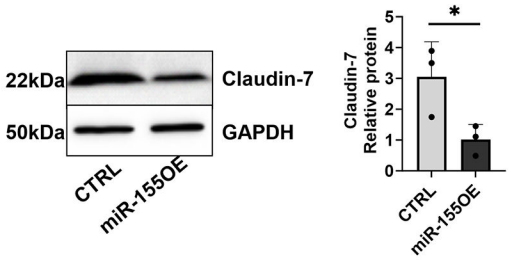

Relative protein expression (GAPDH)	miR-155OE Fold Change ± SEM	Significance
Claudin-1	0.71 ± 0.16	n.s.
Claudin-4	0.01 ± 0.00	n.s.
Claudin-7	1.02 ± 0.28	p≤0.05

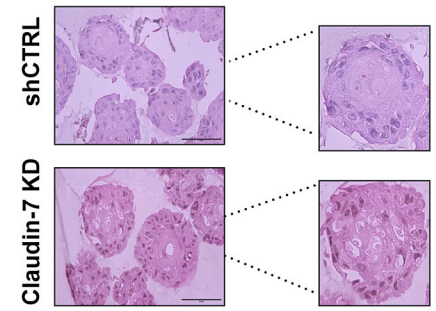

Figure 5: MiR-155–5p overexpression attenuates CLDN7 expression and localisation in esophageal epithelial organoids.

(A) Schematic showing normal esophageal organoid culture development. (B) qRT-PCR of the key tight junction molecules of the esophagus showed a significant decrease in *OCLN* and *CLDN7*. Western blots of whole cell protein isolated from miR-155OE organoids displayed (C) attenuated claudin −7 expression. (D) H&E staining shows dilated intracellular-like spaces evident within the basal region of miR-155OE organoids. Immunofluorescent staining shows perturbed claudin-7 localisation in miR-155OE organoids, note the attenuated peri membranous staining of claudin-7 within the miR-155OE organoids compared to controls (E) Representative H&E staining of Claudin-7KD and shRNA control organoid showing dilated spaces and in Claudin-7KD compared to controls. (F) Claudin-7 promoter showing putative binding sites for transcription actors HNF4α and PU.1 of which are predicted miR-155 targets. Data was analysed for significance using a Students' t test comparing controls. *P < 0.05, **P < 0.01, ***P < 0.001. Data are presented as means ± SEM and represent 3 experimental repeats.

Table 1.

Patient demographics examined by *in situ* hybridisation.

Patient demographics investigated by *in situ* hybridization				
Uninflamed control = 6, Active EoE = 6, Inactive EoE = 6				
	Mean Age	**Male %**	**Female %**	**Peak Eos/HPF**
Uninflamed Control	12.5 ± 1.2	33.3	66.67	0 ± 0
Active EoE	11 ± 1.2	83.3	16.67	34.6 ± 7.5
Inactive EoE	6 ± 1.1	100	0	1.17 ± 1.17